Dynamic Fragmentation of Concrete

Contents

Dynamic Fragmentation of Concrete

Dmitriy Kats and Kevontrez Jones

ABSTRACT: The dissipation of energy due to crack propagation within concrete was analyzed using a computational fracture model. This was modeled as a bar under uniform traction (with a uniform strain rate). The model was a 1D finite element beam with cohesive elements dynamically inserted in order to model the fracture. The simulation was modeled using codes written in Matlab where cohesive elements were dynamically inserted when a critical strength had been reached. These cohesive elements model the damage profile of the material and ultimately define failure. The influence of the strain rate on fragmentation was also investigated. Validation was made through energy conservation and comparison to experimental findings. The results with respect to strain rate influences agree with what was expected and conservation of energy confirms the validity of the numerical approach

KEYWORDS: *Dynamic Brittle Fragmentation, Cohesive Zone, FEM*

I. Introduction

Concrete is one of several materials commonly used for structural applications, which has significant initial porosity. Hence, when subjected to an extreme loading the cracks from the initial porous regions can propagate at high speeds and coalescence to form fragments, which can move and impact each other. Not only is failure of concrete catastrophic, but it has been seen that the on average concrete deviates from the general predictions of fracture mechanics [Bažant 1985].

For these reasons and several others, the fracture mechanics of concrete has been greatly studied. In the present study, the finite element method was used to solve for the fragmentation of a 1D concrete beam that was subjected to a uniaxial strain rate. This was done using a highly accepted cohesive law that describes the strain softening and damage in concrete. From this study, the author's knowledge of both fracture mechanics and the finite element method greatly increased, and it was an overall rewarding experience.

II. Methodology

A. Model Description

A cohesive zone model was used to model the fragmentation of a 1D bar under different strain rates. The bar was discretized using lumped mass at each node and an explicit central difference scheme is used to model the dynamics.

The equation of motion is $\boldsymbol{\nabla} \cdot \boldsymbol{\sigma} = \rho \ddot{\boldsymbol{u}}$, where ρ is the density and $\ddot{\boldsymbol{u}}$ is the second time derivative of the displacement (acceleration).

The equation of motion is discretized using equations (1) - (3), which were suggested by [Hughes 2000].

$$\boldsymbol{u}_{n+1} = \boldsymbol{u}_n + \boldsymbol{v}_n \Delta t + \boldsymbol{a}_n \frac{\Delta t^2}{2} \tag{1}$$

$$\boldsymbol{a}_{n+1} = \boldsymbol{M}^{-1}(\boldsymbol{F}) \tag{2}$$

$$\boldsymbol{v}_{n+1} = \boldsymbol{v}_n + \frac{\Delta t}{2}(\boldsymbol{a}_n + \boldsymbol{a}_{n+1}) \tag{3}$$

Here $\boldsymbol{u}$ is the displacement, $\boldsymbol{v}$ is the velocity, and $\boldsymbol{a}$ is the acceleration. The time step is taken as 0.1 of the critical time step for stability. The mass matrix, $\boldsymbol{M}$, is lumped mass at the nodes. The

force vector, ***F***, takes into account the point forces and internal forces due to the cohesive traction law.

The initial condition, as seen by equation (4), is a linear scaled velocity based of the strain rate and the boundary conditions are constantly pulling the bar in opposite directions. The full description is in can be seen in [Vocialta 2015] but they essentially the same as equations (4) and (5).

Initial Condition:

$$v(x, t = 0) = \dot{\varepsilon}\left(x - \frac{x_{max}+x_{min}}{2}\right) \tag{4}$$

Boundary Condition:

$$\delta(x,t) = \begin{cases} -\frac{\dot{\varepsilon}\, tL}{2} \text{ on leftmost node} \\ \frac{\dot{\varepsilon}\, tL}{2} \text{ on rightmost node} \end{cases} \tag{5}$$

The typical linear cohesive zone model as described by [Vocialta 2015] was used with dynamic parameters for comparison to the spall experiments [Schuler 2006]. A bilinear cohesive zone model was also used to describe the cohesive traction. When the critical cohesive strength, σ_c, is exceeded then the traction law turns on and stays on for the entire simulation. After the cohesive element is fully damaged then it cannot support tension loads while it still can support compressive loads. The bilinear cohesive zone model is as drawn in Figure 1.

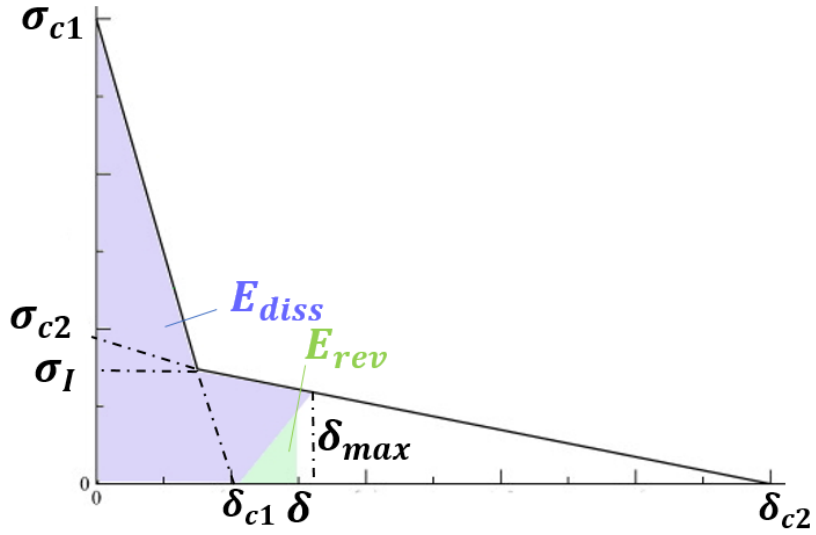

Figure 1: Bilinear cohesive zone model

In Figure 1, σ_{c1} is the critical stress of the material, δ_{c2} is the critical crack width, σ_I is the stress at the intersection of the two linear lines, and σ_{c2} and δ_{c1} are simply the stress and the crack width associated with the linear lines leading to the critical crack length (δ_{c2}) and critical stress (σ_{c1}), respectively. In order to use the bilinear softening curve, the opening size, δ, needs to be used to calculate the traction using equation (6).

$$T(\delta, \delta_{max}, i) = \begin{cases} \sigma_{ci}\left(1 - \frac{\delta}{\delta_{ci}}\right) & \text{for } \delta = \delta_{max} \\ T_{max}\frac{\delta}{\delta_{max}} & \text{for } 0 \le \delta \le \delta_{max} \\ 0 & \text{for } \delta < 0 \end{cases} \tag{6}$$

(i = 1 for 1st softening curve, i = 2 for 2nd softening curve)

This formula is based off the work of [Vocialta 2015]. After the opening size exceeds δ_{c2} then the cohesive element is fully broken and it can no longer sustain any traction. However, no contact is considered.

The energy is calculated the same way as described by [Vocialta 2015], which is shown in equations (7) and (8). Along with the energy description, equation (9) describes a damage law that is used to account for decohension. The dissipated and reversible energies need to be calculated in a modified way based on the updated area of the triangles as shown in Figure 1 above.

$$E_{diss} = \frac{1}{2}\sigma_c \delta_{max} \tag{7}$$

$$E_{rev} = \frac{1}{2} T \delta \tag{8}$$

$$D = \min\left(\frac{\delta_{max}}{\delta_c}, 1\right) \tag{9}$$

B. Bilinear Cohesive Zone Parameters

According to [Bažant 2002], the parameters for the bilinear cohesive law described in the previous section can be defined as the following:

$$\sigma = f(w) \tag{10}$$

$$G_f = \frac{{f'_t}^2}{2\sigma'_0} = \frac{{w_0}^2 \sigma'_0}{2}; \quad \sigma'_0 = \frac{df(0)}{dw} = \frac{{f'_t}^2}{2G_f} \tag{11}$$

$$G_F = 2.5 G_f \tag{12}$$

$$w_f = \frac{2}{\psi f'_t}\left[G_F - (1-\psi)G_f\right] \tag{13}$$

For the case of concrete a possible parameter is $\psi = 0.25$ [Bažant 1998, Rokugo 1989, and Wittman 1988] which leads to these parameters (also shown in Figure 2):

$$\rightarrow w_f \approx \frac{14 G_f}{{f'}_t} \quad or \quad w_f \approx \frac{5.6 G_F}{f'_t} \tag{14}$$

$$\rightarrow w_0 = \frac{w_f}{7} \tag{15}$$

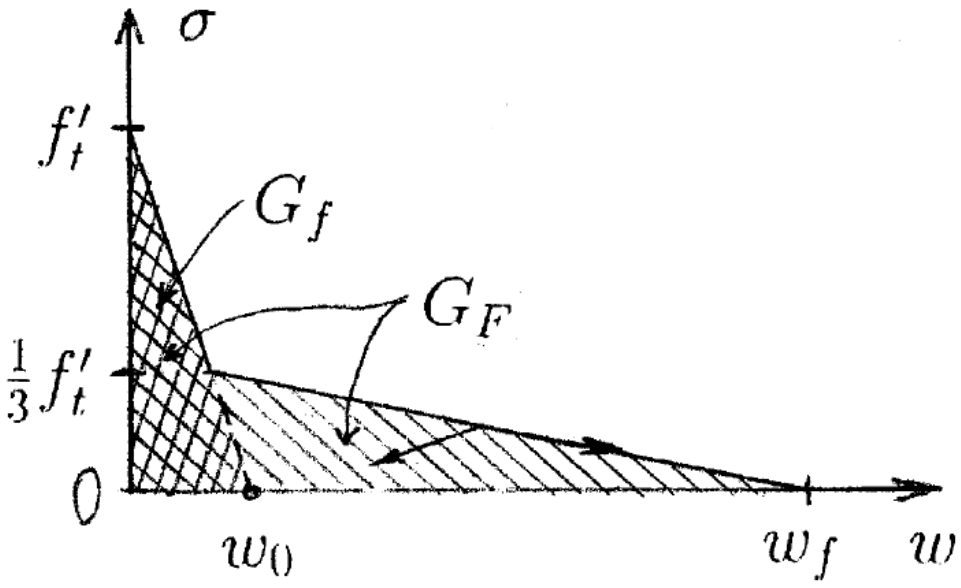

Figure 2: Bilinear cohesive softening curve for concrete [Bažant 2002]

III. Results

A. Effect of Strain Rate on Fragments

The methods outlined in the previous section are used to investigate the effect that the strain rate has on both the size of the fragments and the frequency that they are formed. In both cases, various strain rates ranging from $25s^{-1}$ and $200s^{-1}$ are applied to a bar of length 250mm and the material properties outlined in Table 1. The mesh size consisted of 9000 elements and the critical stress for the mesh was determined by using a Weibull distributed of the tensile strength of the material across the elements. By using this distribution for the critical stress, numerical instabilities due to stress localizations are eliminated. Also, the simulation ran for 18000 time steps of 0.1s.

Table 1: Material Properties used for Simulations

Density (kg/m^3)	Young's Modulus (GPa)	Tensile Strength (Mpa)	Total Fracture Energy (N/m)
2320	25.5	3.5	32

As seen from Figure 3, the results from the numerical approach was in good agreement with the physical phenomena that is expected. In terms of the number of fragments that appear, it was seen that in general as the strain rate is increased, there are more fragments. This indicates that the beam is being broken apart into more pieces. Also, when a strain rate of $50s^{-1}$ or smaller was applied there were no fragments observed, and hence such strain rates are too small to break the concrete material for this model for this many time steps. A longer simulation produces more framgnets. Although the general idea of the frequency of fragments increasing with load is expected to be seen, one interesting result is the sharp increase in fragment size seen when a strain rate of $125s^{-1}$ is applied. One would expect the value to lay between those of $100s^{-1}$ and $150s^{-1}$, the authors believe it to be attributed to some random numerical instability problem that arises from this particular case.

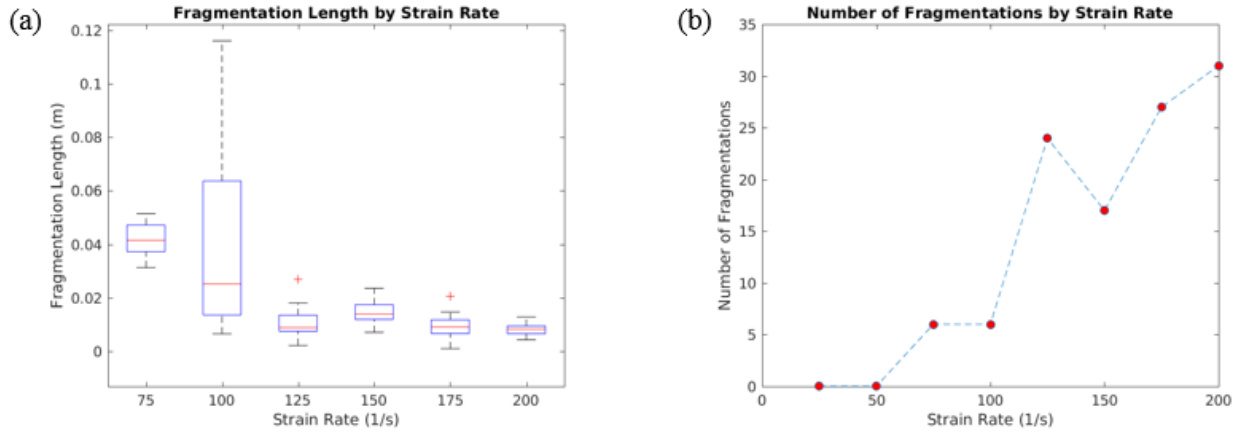

Figure 3: Plot of the Fragmentation length vs Strain Rate (a) and the Number of Fragments vs Strain Rate (b)

Along with the increase in number of fragments, it is seen that the range of the fragment sizes decreases as the strain rate is increased. Instead of the average fragment decreasing, they are slowly localizing to a single size. Hence for the higher strain rates, there are more fragments, but each fragment is relatively the same size as the others. Once can image this phenomena as the

concrete material beginning to crumble into several pieces as the strain rate at high strain rates, whereas it simply separates/splits at lower strain rates.

B. Mesh Convergence Study

A mesh convergence study was completed for a strain rate of $\dot{\varepsilon} = 200/s$. Four simulations were done at a particular number of elements with different Weibull distributed random σ_c as was done by [Vocialta 2015]. A linear softening curve was used for the mesh convergence study. The material data came from [Schuler 2006]. Since the critical strength distributions change for each simulation there isn't perfect convergence as seen in Figure 3. However, above 5000 elements the number of fragments doesn't vary too much so 9000 elements were used for the simulations that had strain rates below the one tested here.

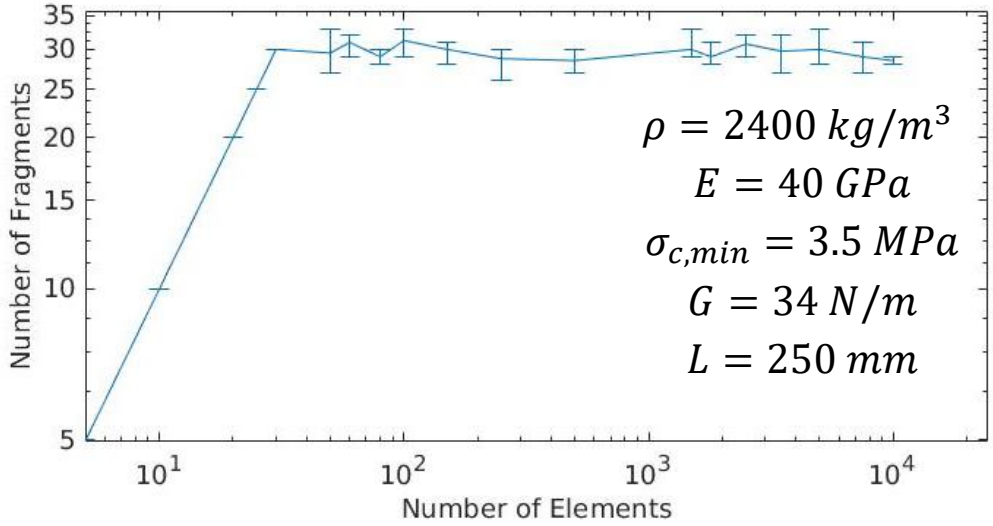

Figure 4: Mesh Convergence study at $\dot{\varepsilon}_0 = 200/s$

C. Energy Conservation

The energy is conserved throughout the simulations. One example of the energy plot is seen in Figure 5. The dissipated and reversible energies are due to the cohesive elements. The external work comes from the boundary conditions. The other energies are the typical energies found in a dynamic finite element simulation.

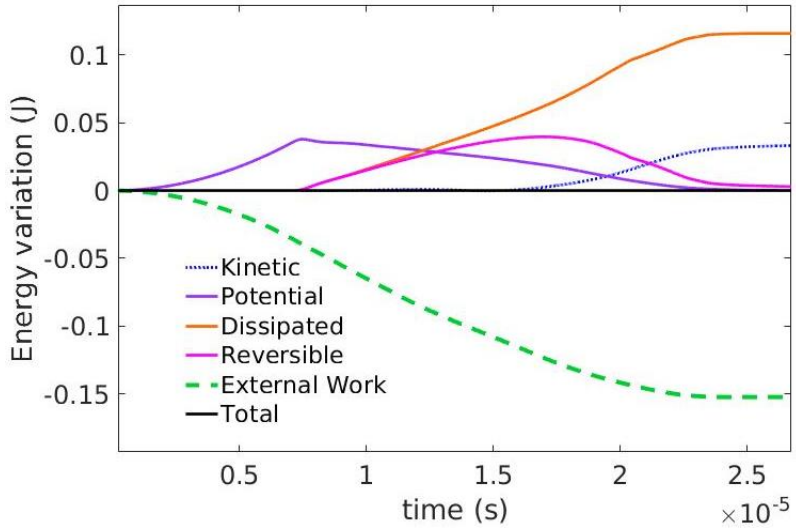

Figure 5: Conservation of Energy

D. Comparison to Spall Experiments

In [Schuler 2006], there was a description of spall experiments on concrete where a Split-Hopkinson pressure bar was used to study the fragmentation of concrete under different strain rates. The results are written below in Table 2:

Table 2: Experimental spall results [Schuler 2006]

Sample	$L_1(mm)$	$L_2(mm)$	$L_3(mm)$	$L_4(mm)$	$E_{dyn}(GPa)$	$\sigma_{fdyn}(MPa)$	$G_{fdyn}(J)$	$\dot{\varepsilon}(1/s)$
SHB 17	124	38	76	-	37.7	16.0	4.57	59.1
SHB 25	109	25	45	68	39.3	18.7	6.01	72.1
SHB 26	133	33	79	-	40.0	17.1	7.83	72.5

The original length of the bar was 250 mm and by the summation of the length (L_i is the length of the i^{th} fragment) of the fragments one can see that only the largest fragments were recorded.

To compare to these experiments the dynamic values of the strength and fracture energy were inputted into the linear softening curve. A critical cohesive strength distribution is needed for the simulation which should represent the number of defects in the actual material. It was found that the numerical results, listed in table 3, were dependent on the location of these defects so only some of the simulation results were close to the experimental results. However, if the average fragment were compared then there would likely be good agreement.

Table 3: Numerical Results for Comparison to Experiments

Numeric Experiment	$s_{ave}(mm)$	$L_{max}(mm)$	$\dot{\varepsilon}(1/s)$
SHB 17 (CZM)	35.72	54.42	59.1
SHB 25 (CZM)	25.00	49.00	72.1
SHB 26 (CZM)	31.25	50.14	72.5

IV. Conclusion

Dynamic fragmentation of concrete was investigated by using a bilinear cohesive law and general damage using a finite element method approach. Acceptable mesh convergence was seen above 5000 elements, while 9000 elements were used for the numerical studies. The number of fragments increased with elongation rate and the range of fragment lengths decreased with elongation rate.

The implementation was shown to be numerically sound, via conservation of energy. Also, the results match with expected trends. However, the biggest limitation in the work was that it was in one dimension. Two dimensions are needed to adequately model any real physical phenomena. Due to the large addition of complexity when using a 2D implementation instead of 1D, the program would have to be extended for parallelization or else it would be greatly limited in the number of elements that could be used.

Through this project, the authors learned about how to implement a cohesive model into a finite element method problem, and they got better at coded finite elements. This is essential knowledge because both the authors are currently PhD students involved in a research group that works extensively with finite element analysis. One of the things that was interesting in working on this project was finding a large amount of literature that has been written regarding the fracture of concrete. In fact, a one of the authors that routinely had publications in the topic was Dr. Zdeněk Bažant, who's a here professor at Northwestern University. So it was pretty neat surging through some of his older bodies of work on the topic. Another interesting component of

this project was looking into how others approached the challenge of implementing a similar numerical approach as the one used in this study to 2D problems. The 2D problem is vastly more complicated than that of the 1D, in that high-performance computation is necessary to avoid script limitations.

References

[Bažant 1985] Bažant,Z. P., “Mechanics of Fracture and Progressive Cracking in Concrete Structures," Fracture Mechanics of Concrete: Structural Application and Numerical Calculation, eds. G.C. Sih and A. Ditommaso, Martium Nijhoff, 1985, 1-94.

[Bažant 1998] Bažant Z.P., Planas, J.,”Fracture and Size Effect in Concrete and other Quasibrittle Materials,” Boca Raton, FL: CRC Press; 1998.

[Bažant 2002] Bažant, Z.P.,”Concrete Fracture Models: Testing and Practice,”*Engineering Fracture Mechanics* 69: (2002) 165-205.

[Hughes 2000] Hughes, T. J., 2000. *The Finite Element Method: Linear Static and Dynamic Finite Element Analysis*. Courier Corporation.

[Rokugo 1989] Rokugo, K., Iwasa, M., Suzuki, K., Koyanagi, W., “Testing Methods to Determine Tensile Strain-Softening Curve and Fracture Energy of Concrete,” eds. Mihashi, H., Takahashi, H., Wittman, F.H., *Fracture Toughness and Fracture Energy: Test Methods for Concrete and Rock*, Rotterdam: Balkema; 1989. 153-163

[Schuler 2006] Schuler, Harald, Christoph Mayrhofer, and Klaus Thoma. "Spall experiments for the measurement of the tensile strength and fracture energy of concrete at high strain rates." *International Journal of Impact Engineering* 32.10 (2006): 1635-1650.

[Vocialta 2015] Vocialta, M., Molinari, J., 2015. Influence of internal impacts between fragments in dynamic brittle tensile fragmentation. *International Journal of Solids and Structures* 58, 247-256.

[Wittman 1988] Wittman, F.H., Rokugo, K., Brühwiller, E., Mihashi, H., Simopnin, P., ”Fracture Energy and Strain Softening of Concrete of Concrete as Determined by Compact Tension Specimens,” *Material Struct* 21 (1988) 21-32.